

SURFACE OZONE IN THE INDUSTRIAL CITY OF CHELYABINSK, RUSSIA

Tatyana G. Krupnova^{*1}, Olga V. Rakova¹, Valeria I. Simakhina¹, Ekaterina A. Vykhodtseva², Valeriy M. Kochegorov²

¹Institute of Natural Sciences and Mathematics, South Ural State University, 76 Prospect Lenina, Chelyabinsk, 454080, Russia

²Chelyabinsk Center for Hydrometeorology and Environmental Monitoring, Federal Service for Hydrometeorology and Environmental Monitoring (Rosgidromet), 15 Vitebskaya st., Chelyabinsk, 454080, Russia

***Corresponding author:** krupnovatg@susu.ru

Received: April 21st 2024 / Accepted: November 27th 2024 / Published: December 31st 2024

<https://doi.org/10.24057/2071-9388-2024-3364>

ABSTRACT. This work studies the variations in daily and seasonal concentrations of surface ozone (O_3), and nitrogen oxides (NO and NO_2) as its precursors in Chelyabinsk, a large industrial city in Russia. A monitoring station located outside the zone of influence of large industrial and transport local sources of air pollution was chosen for the research. The research was carried out during 2019, which can also be considered as a “background” period, because in 2020, during the COVID-19 lockdown, there was a decrease in concentrations of precursors. However, in 2022–2024 concentrations of precursors increased due to increased production capacity. Daily O_3 variations are characterized by three peaks that correlate with changes in concentrations of nitrogen oxides (NO_x) determined by peak loads and emission intensity of thermal power stations. There are two seasonal peaks of surface O_3 concentrations. The spring peak in March is caused by natural processes. In March 2019, an advection of an air mass with different properties and gas composition was observed from areas with powerful sources of precursor gases or saturated with O_3 from the south (areas in Kazakhstan). During episodes of high O_3 levels, Chelyabinsk was located on the crest of a cyclone, in the warm sector, where low-level jets formed. The summer maximum of surface O_3 in June was caused by photochemical reactions during anticyclones and prolonged inversions.

KEYWORDS: surface ozone, nitrogen oxides, temperature inversion, low-level jets

CITATION: Krupnova T. G., Rakova O. V., Simakhina V. I., Vykhodtseva E. A., Kochegorov V. M. (2024). Surface Ozone In The Industrial City Of Chelyabinsk, Russia. *Geography, Environment, Sustainability*, 4(17), 223–234
<https://doi.org/10.24057/2071-9388-2024-3364>

ACKNOWLEDGEMENTS: This study was supported by grant from the Russian Science Foundation, project 24-27-20017 and Chelyabinsk oblast.

Conflict of interests: The authors reported no potential conflict of interest.

INTRODUCTION

Surface ozone (O_3) is one of the most dangerous urban air pollutants, having caused several hundred thousand premature deaths and tens of millions of asthma attacks worldwide (Zhang et al. 2019). O_3 is necessary in the stratosphere but undesirable in the troposphere because it reacts with many compounds to form oxygen-containing organic substances and particles. Humans are exposed to O_3 mainly through inhalation, but cutaneous reactions have also been reported (Salonen et al. 2018). Being highly reactive, it can cause a 25% increase in the rates of skin cancer (Rawat and Matta 2021). In the troposphere, O_3 is categorized as a secondary pollutant because it is not emitted directly but is synthesized through chemical reactions from precursors (Nuvolone et al. 2018). Its sources in urban air are debated. Despite the large number of studies on surface O_3 in cities, there is practically no research focusing on O_3 concentrations in Russian industrial cities.

Complex photochemical reactions between nitrogen oxides (NO_x) ($NO+NO_2$) and volatile organic compounds (VOCs) form ozone (Belân 2010; Nguyen et al. 2022). Changes

in VOCs, NO , and NO_2 concentrations, as well as weather conditions, influence surface O_3 concentrations (Ouyang et al. 2022; Di Bernardino et al. 2023; Wang et al. 2023). Industry, transport, and power plants produce NO_x . The contribution of different sources to VOCs varies considerably from city to city and region to region; these can be vehicle and industrial emissions as well as emissions from urban vegetation.

Isoprene (McGenity et al. 2018) and terpenes (Rosenkranz et al. 2021) are the main VOCs produced by plants. The effect of isoprene emissions on O_3 formation in cities is well known (Watson et al. 2006). Studies showed that some types of trees emit significantly more isoprene (e.g., poplar, oak) (Simon et al. 2019). In south Shanghai, biogenic VOCs are the major precursors of O_3 . This mechanism is defined as O_3 production in the area leeward of the isoprene source in forests (Geng et al. 2011). The increase in O_3 concentration in the Seoul metropolitan area is also largely due to biogenic isoprene emissions (Lee et al. 2014; Kim et al. 2016). However, the major sources of VOCs are coal combustion and coking. For example, a study from Taiyuan, Shanxi Province, China, showed that the main sources of VOCs included coal and biomass combustion (33%) and coking sources (28%). Vehicle

and biological emissions were 14% and 7%, respectively (Ren et al. 2021). In some large industrial cities, without oil and coke production, transport is the main source of VOCs (Xie et al. 2021).

There is no doubt that O_3 -VOC- NO_x concentrations are closely interrelated. VOCs are oxidized in the troposphere forming O_3 . However, the more NO_x released, the less O_3 produced, since NO_x titrates O_3 . Thus, we increase O_3 by reducing NO_x emissions. Recent data, however, have shown that even if all anthropogenic VOC emissions are reset to zero, the amount of O_3 will still be significant (Colombi et al. 2023). According to Colombi et al. (2023), decreasing VOC emissions would reduce the amount of O_3 in South Korea, but concentrations would remain above 80 ppbv even if all anthropogenic emissions from South Korea and China were zeroed out. The East Asian atmospheric background, determined by zeroing out all anthropogenic emissions over East Asia, is very high at 55 ppbv, which means that the 60 ppbv air-quality standard in South Korea is out of reach without dealing with the cause, which is still not clear.

Surface O_3 concentrations and their relationship with meteorological conditions, inversion layers, and heat islands should be studied to improve the understanding of the physicochemistry of these phenomena and to develop and evaluate strategies for improving air quality. Recent studies have shown that traditional greening strategies (Knight et al. 2021) and white roofs (Fallmann et al. 2016) have little efficacy.

Until recently, the concentration of surface O_3 has been the subject of little attention in Russian cities. In recent years, the ongoing economic digitalization and the implementation of smart cities have led to the emergence of online air quality monitoring systems in many large cities in Russia, including the monitoring of surface O_3 concentrations. Several Russian research groups are working on surface O_3 monitoring (Berezina et al. 2020; Simakina et al. 2020; Chubarova et al. 2021; Thorp et al. 2021; Andreev et al. 2021; Virolainen et al. 2023). One of the latest reviews (Andreev et al. 2022) showed that during 2021, the average daily O_3 concentration exceeded the maximum permissible concentration (MPC) for most of the year for all observation sites (17 stations), and at some stations it is double or even triple the MPC. Anticyclonic conditions in summer observe the maximum concentration in Moscow and St. Petersburg, while some stations, like Obninsk, observe maximum concentrations in March and even December, a phenomenon that remains unexplained (Andreev et al. 2022).

A study of the background O_3 concentration in Siberia in an area devoid of anthropogenic influence by Moiseenko et al. (2021) was conducted at the Zotino Tall Tower Observatory (ZOTTO) at a remote station in Central Siberia, commissioned in October 2006 as part of a joint project of the Max Planck Institute for Biogeochemistry, Jena, Germany, and the Sukachev Institute of Forestry, Siberian Branch of the Russian Academy of Sciences, Krasnoyarsk (Russia). In March and April, ZOTTO recorded the highest amount of O_3 in background conditions with low-pollution. This amount dropped significantly in May and reached a plateau by June for the observation period from 2006 to 2014. There is data on spring maxima from at least seven more stations in Russia, which are usually background or suburban stations (Andreev et al. 2022).

A more comprehensive analysis of O_3 formation in specific cities in Russia is required. Russian industrial cities are unique urban ecosystems. The vast concentration of industrial enterprises defines their development and ecological peculiarities. This paper studies, for the first time, the patterns of annual and daily variation of surface O_3 concentrations in a typical Russian industrial city, Chelyabinsk.

METHODOLOGY

Study area and observation station

Chelyabinsk is located on the geological boundary of the Urals and Siberia, in the Asian part of Russia, on the eastern slope of the Ural Mountains, on both banks of the Miass River (the Tobol River basin). The city's relief is mildly hilly. The climate is moderately continental.

Chelyabinsk is the administrative center and largest city of the Chelyabinsk region, Russia. It is the seventh-largest city in Russia with a population of over 1.1 million people. Chelyabinsk is a typical Russian industrial city, with an area of 530 km². It contains several of the largest metallurgical enterprises in Russia, including the country's only zinc plant, the largest steel foundry, coke and chemical enterprises, a pipe-rolling plant, a steel smelter for the production of ferro-manganese, ferro-chrome, and electrodes, and several enterprises for the production of mineral wool. Chelyabinsk is a major transport hub, with an international airport, a railway station, and several state highways. In addition to cargo and personal transport (many families in the city have more than one car), Chelyabinsk has a well-developed public transport network, including bus, tram, and trolleybus fleets, and a new metro is under construction. For the analysis, we used the data from the official monitoring station of the Russian Federal Service for Hydrometeorology and Environmental Monitoring (Roshydromet). The service operates independently from the local city authorities, and all laboratories have accreditation certificates for chemical and analytic measurements and the monitoring of air conditions. O_3 content monitoring has been conducted in the city since 2019, but measurements of surface O_3 content were not mandatory until recently and were experimental; therefore, data were not available for all monitoring stations and not for all time periods.

Monitoring stations can only be categorized roughly. In Russian industrial cities, there is no division into residential, industrial, and commercial zones. As a result, industrial enterprises can be found in the city center, and one of the world's largest zinc plants is located in the central area of Chelyabinsk. In the north of the city, there is an industrial area with Russia's largest steel smelting plant.. Many employees prefer to live close to work, so there are large residential areas in the neighborhood, which are interspersed with commercial property. The monitoring stations have been described in detail by Krupnova et al. (2020).

Direct emissions have minimal impact on two background monitoring stations. However, one of them is adjacent to a large urban forest with relic pine trees and exposed to a busy nearby highway. So, we chose the other as the urban background (UBG) station (Fig. 1).

We chose 2019 as the conditional background year for this paper because it best reflects the city's ecosystem, characterized by stable traffic flows and the work of industrial enterprises throughout the year. From 2020, the city was affected by social and political issues and was marked by COVID-19 lockdowns, which caused remote work and studies in 2021, and therefore, changes in the traffic flows of personal and public transport. In 2022, Russia came under sanctions, which led to a temporary decrease in production and consequently a decrease in emissions of dust and NO_x . In response, the economy was oriented toward domestic markets, which was followed by an increase in production to record levels. All these processes are difficult to take into account when analyzing the situation. Production volumes are classified information, as the enterprises in the city are related to national security. These social and economic processes in 2020–2022 had

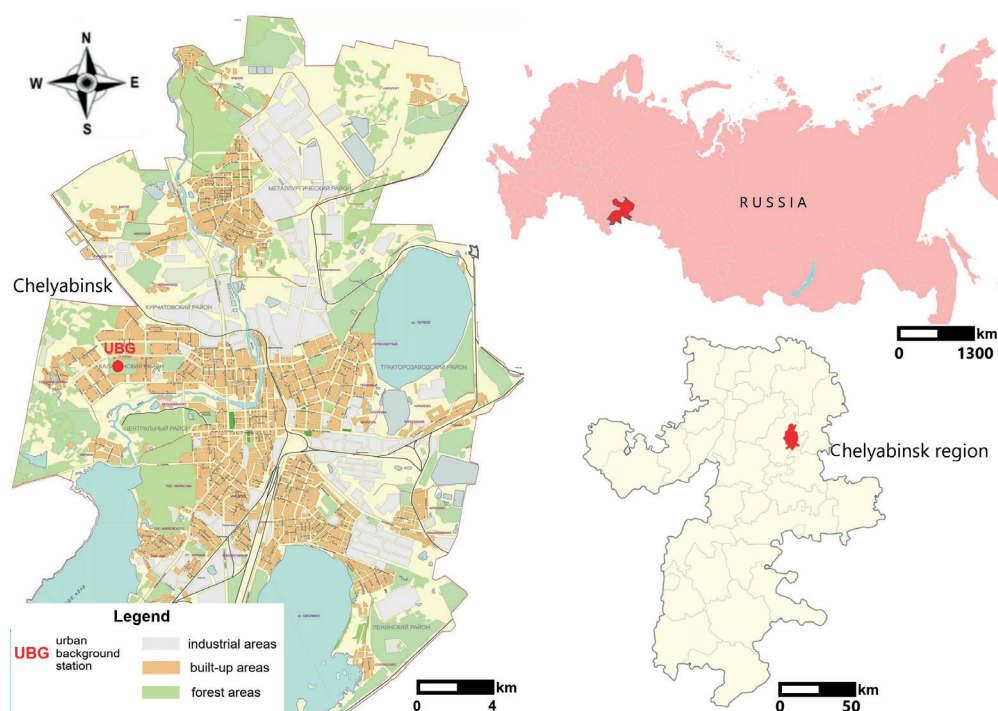


Fig. 1. Map of study area and observation station location

a significant impact on NO_x and dust emissions affecting the surface O_3 cycle. Therefore, we chose 2019 to analyze typical daily and seasonal O_3 variations for Chelyabinsk, as well as correlations with NO_x and meteorological conditions. We used data from the Roshydromet server. Pollution monitoring is continuous with measurements every 20 minutes (72 per day). In addition, we analyzed episodes of high O_3 concentrations at the background station.

Description of the data and instrumentation

Hourly averaged meteorological parameters were captured by a meteorological station (Davis Instruments Vantage Pro2, USA). Gases were measured by a set of commercial instruments. O_3 was measured by an ultraviolet photometric analyzer (OPTEC, F-105, Russia), with detection limit of 1 ppbv (10 s average). We performed calibration checks using NIST-traceable O_3 standards.

NO and NO_2 were monitored using a chemiluminescent analyzer (OPTEC, R-310 A, Russia). We calibrated this analyzer weekly with certified NO compressed gas standards and dynamic dilution calibrators, as well as monthly with NO gas standard dilution and gas phase titration. The results were processed using Microsoft Excel 2013 and IBM SPSS 27.0 software.

Measurements with the altitude temperature profiler MTP-5 (Russia) provided the parameters for temperature inversions.

The analysis of synoptic situations during episodes of increased O_3 concentrations was carried out by analyzing charts of the absolute and relative topography at the level of 300, 850, 925 hPa (at observation times of 00:00 and 12:00 UTC), maps of surface analysis, and annular weather maps (at 00:00, 03:00, 06:00, 09:00, 12:00, 15:00, 18:00 UTC) available in the archive of the Chelyabinsk Central Hydrometeorological Service. To assess large-scale atmospheric circulations, data from a report by the Russian Hydrometeorological Center on the main features of atmospheric and weather conditions in the northern hemisphere was used.

RESULTS AND DISCUSSION

Dependence of surface O_3 concentrations on season

Fig. 2 shows monthly variation of O_3 , NO , NO_2 concentrations in 2019.

Fig. 2 shows that the concentration of O_3 increases from January to March. The first local maximum is observed in March, followed by slow growth, and the main maximum is observed in June. Then the concentration of O_3 gradually decreases, reaching a minimum in December. The concentration of NO is maximum in February–March, and then it gradually decreases. There is a NO minimum in July. After that, NO gradually increases until December. Similarly, NO_2 reaches its peak in February. In June–August, there is a NO_2 minimum. After that, NO_2 gradually increases until December. The main sources of NO_x are metallurgy, thermal power plants, and motor transport. Most metallurgical production is year-round; therefore, they do not affect seasonal changes in NO_x emissions. The central heating season begins in October and ends in April in Chelyabinsk. The coldest days are often in January and February when heating capacities are at maximum. This is the likely reason for the observed seasonal change in NO_x concentrations. In addition, in recent years, during the winter, people have often used remote ignitions to turn on and warm up car engines — often for 15–20 minutes several times a day. This leads to an increase in NO_x emissions. In new residential districts of Chelyabinsk there are local central heating systems that can be used at any time, even on cold summer days, with an uncomfortable decrease in temperature in rainy weather in early autumn. O_3 synthesis begins to increase from March, reaching a maximum in July along with an increase in solar radiation activity (Fig. 3).

The March local maximum is counterintuitive since solar radiation is not yet very high (Fig. 3), but the amount of NO_x remains high. As noted in the introduction, the spring maximum described in a large number of works is typical for the entire Eurasian territory. It is not associated with local sources, but rather reflects natural processes. There is convincing evidence that, unlike the summer maximum, which is associated with photochemical O_3 generation, the spring maximum is associated with atmospheric dynamics. During the periods under study, advection of an air mass with different properties and gas composition was observed from areas with

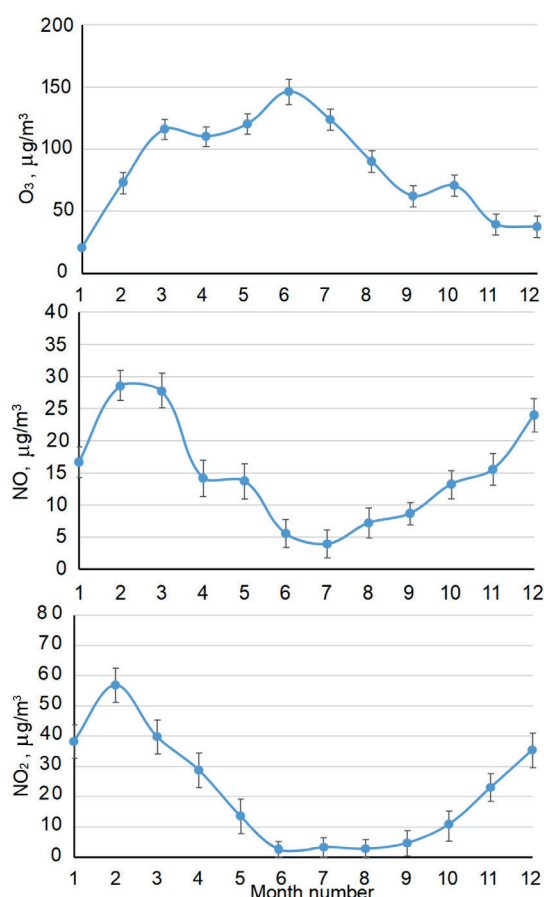


Fig. 2. Monthly variation of O_3 , NO , NO_2 concentrations ($\mu\text{g}\cdot\text{m}^{-3}$) in 2019

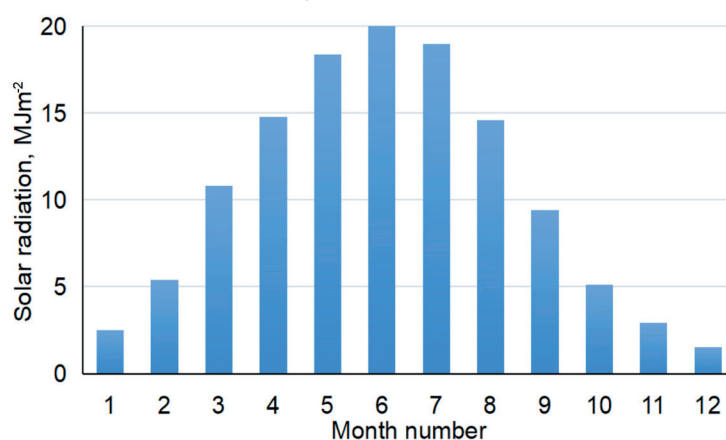


Fig. 3. Monthly values of solar radiation ($\text{MJ}\cdot\text{m}^{-2}$) in 2019

powerful sources of precursor gases or saturated with O_3 from the south (areas of Kazakhstan, Central Asia), or from the west, which is transferred by a southwest flow enveloping the Ural Mountains from the south. As an atmospheric front passes, the thermal structure of the atmosphere changes, as does the gas composition. Similar phenomena have been described by Antokhin et al. (2020). Below we consider in more detail two episodes of increased O_3 concentrations in March 2019, caused by the formation of cyclone-induced low-level jets (LLJs).

Dependence of surface O_3 concentrations on the time of day

Fig. 4 shows that NO and NO_2 concentrations are negatively correlated. At 7 a.m., 1 p.m., and 7 p.m., there is a maximum of NO_2 and a minimum of NO . In January and February, at the same times, three O_3 maxima are observed; starting in March, the morning and evening maxima become minima, the daytime maximum persists in all seasons, and a nighttime O_3 maximum appears, which in December is larger

than the daytime one. The main peak in the afternoon hours is associated with solar radiation.

In January and February, long-term surface inversions were almost constant (Table 1), while there was no movement of the air in the inversion layer or air with pollutants circulating under the inversion layer. The upper atmosphere had no vertical supply of O_3 . Almost the entire mass of O_3 was formed as a result of photochemical reactions. The predominant sources of NO_x and VOCs are emissions from thermal power plants and boilers. The fact that NO_x extremes do not align with vehicle peak hours (in Chelyabinsk, 9 a.m. and 8 p.m.) supports this. At 7 a.m., 1 p.m., and 7 p.m., peak loads and emissions from thermal power stations are associated with nitrogen dioxide extremes (Fig. 5).

In March, there was a morning and afternoon O_3 maximum, as well as an evening minimum. In addition to the photochemical mechanism, conditions exist for the vertical supply of O_3 from the upper layers of the atmosphere. Gradually, the daytime maximum becomes

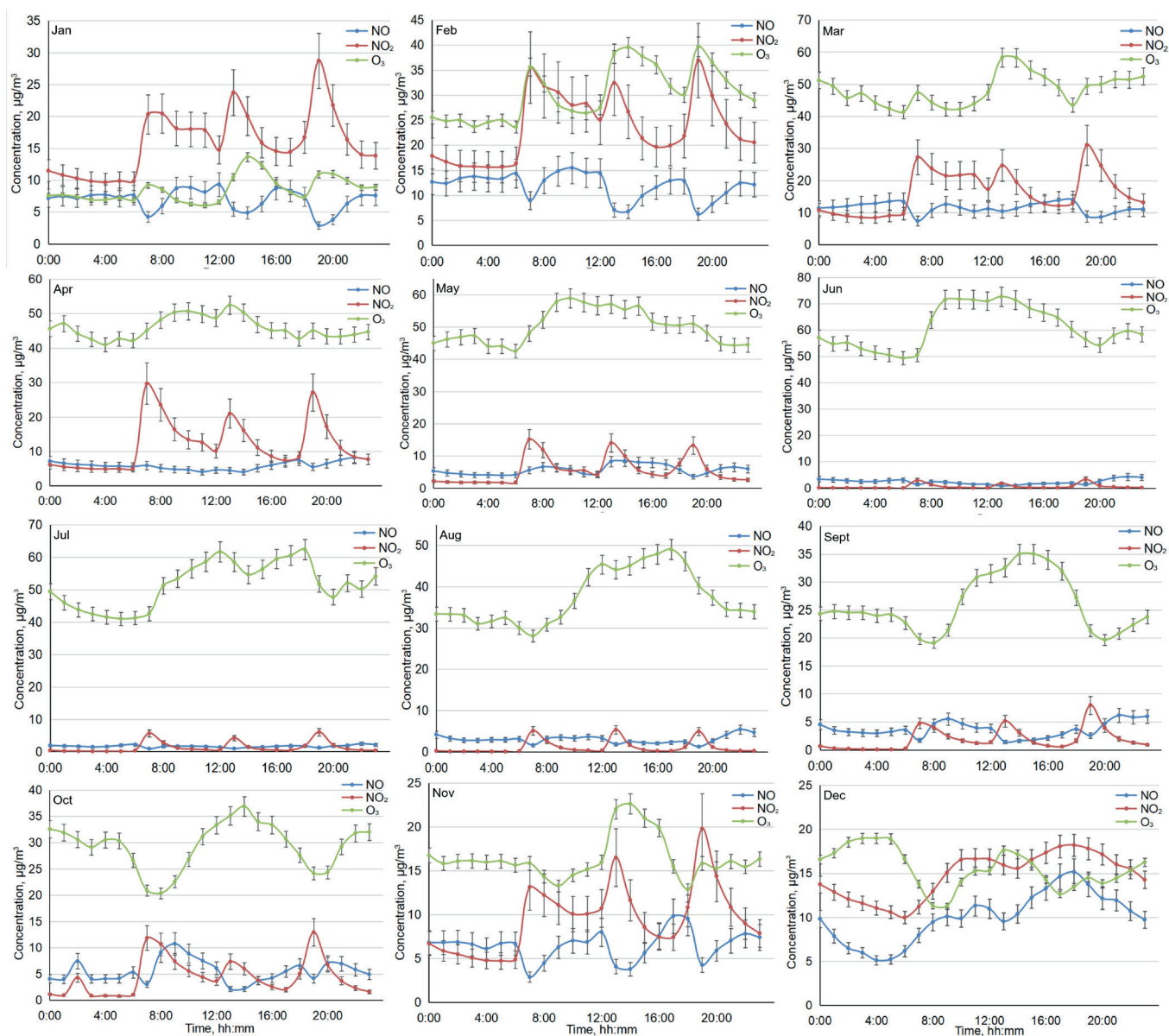


Fig. 4. Hourly variation of NO, NO₂, and O₃ concentrations (µg·m⁻³) during the year

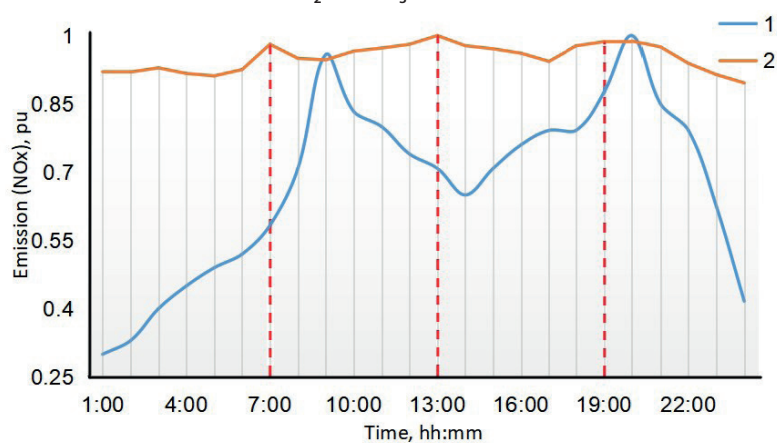


Fig. 5. Relative intensity of emissions from (1) motor vehicles¹ and (2) thermal power stations²

¹ <https://aims.susu.ru>

² <https://purchase.frw.d.energy/monitoring-chtec/>

Table 1. Average duration of inversions in different months

Month	Average duration of inversions, h
January	12
February	13
March	8
April	6
May	6
June	6
July	5
August	5
September	6
October	6
November	7
December	8

more pronounced; in April, a morning minimum and nocturnal increases in O_3 concentration appear. The nocturnal maximum becomes most pronounced from October to December. Nocturnal O_3 enhancement is caused mainly by atmospheric processes, including horizontal transport and vertical mixing. Horizontal transport connects with follow phenomena. At night, the intensity of vehicle traffic decreases, and air masses gradually move into the city, where ground-level O_3 has not been destroyed by anthropogenic emissions. Low-level jet streams include vertical mixing. The O_3 produced by the photochemical reactions during the day provides an abundant O_3 source in the nocturnal residual layer, and atmospheric mixing causes the ozone-rich air in the residual layer to mix into the nocturnal boundary layer, triggering the nocturnal O_3 increase. Low-level jets' turbulence decouples the residual layer from the stable boundary layer, resulting in a decrease in the residual layer's O_3 concentration and an increase in the surface O_3 concentration. By morning, there is a decrease in the concentrations of terrestrial O_3 due to the fact that its supply from the troposphere is minimal since the atmosphere at this time is as stable as possible.

Episodes of high O_3 concentrations

Episode 1

Fig. 6 shows that the surface O_3 concentrations were 90–115 $\mu\text{g}\cdot\text{m}^{-3}$ on March 6 from 3 p.m. to 7 p.m. and 100–120 $\mu\text{g}\cdot\text{m}^{-3}$ on March 7 from 1 a.m. to 9 a.m.

At the 300 hPa level (≈ 9 km), Chelyabinsk region and Chelyabinsk city were located at the periphery of an extensive trough of a near-field cyclone. Flows were observed in a western, southwestern direction of 27–31 $\text{m}\cdot\text{s}^{-1}$ (97–112 $\text{km}\cdot\text{h}^{-1}$). At the level of 850 hPa (≈ 1.5 km), Chelyabinsk was located on the southeastern periphery of a vast trough of a cyclone. The map (Fig. 6) clearly shows the passage of a warm atmospheric front through Chelyabinsk and the Chelyabinsk region, as well as LLJs in the warm sector of the cyclone. At the same time, a sharp increase in air temperature was observed from a night temperature of -12 to a daytime temperature of $+4$ according to the profile on March 6 and $+5.3$ $^{\circ}\text{C}$ on March 7 (at night on March 7, the minimum temperature was about 0 $^{\circ}\text{C}$). In the evening of March 7, with the passage of a

cold front (Fig. 6), the air mass changed again; a decrease in temperatures, an increase and change in wind direction, and a resulting decrease of the O_3 concentration in the surface layer were observed. The high O_3 level in the evening and at night on March 6 and in the morning of March 7 is not the result of local O_3 formation, but is of an advective nature. A warm air mass saturated with O_3 was brought from Central Asia by southwesterly flows. The cyclone-induced LLJs transport O_3 to the ground, where it accumulates. No inversions were observed on March 6 and 7, and there were no obstacles to O_3 penetration into the surface layers.

Episode 2

Another episode of high O_3 concentrations was observed on March 11–12 (Fig. 7). In the two episodes, the synoptic situation is almost identical. At the 300 hPa level (≈ 9 km), the Chelyabinsk region and Chelyabinsk city were on the eastern periphery of the trough of an extensive cyclone, the maximum development of which occurred on March 12. At the level of 850 hPa (≈ 1.5 km) Chelyabinsk, as in episode 1, was located on the south-eastern periphery of a vast trough. Heat was spreading in the atmosphere by south-western flows, a warm front was observed on the 11th and an occlusion front on March 12, and LLJs were also observed in the warm sector. At night, the air temperature was from -2.2 to $+1.5$ $^{\circ}\text{C}$, and during the day it warmed up to $+4$, $+6$ $^{\circ}\text{C}$. High O_3 concentrations were 115–130 $\mu\text{g}\cdot\text{m}^{-3}$ and 80–135 $\mu\text{g}\cdot\text{m}^{-3}$ from 2 p.m. to 7 p.m. on March 11 and from 8 a.m. to 2 p.m. on March 12, respectively. The inversions were characteristic only for the early morning of March 12 and quickly collapsed. The LLJs transported O_3 to the ground.

Episode 3

Tropospheric O_3 concentrations of up to 210 $\mu\text{g}\cdot\text{m}^{-3}$ were recorded during the day from May 8 to 9 (Fig. 8). At the 300 hPa level (≈ 9 km), from May 8, the Chelyabinsk region and Chelyabinsk city were at the crest of increased geopotential; the leading flow was southward from 21–24 $\text{m}\cdot\text{s}^{-1}$ (76–86 $\text{km}\cdot\text{h}^{-1}$), due to the pushing of the high-altitude trough near the polar cyclone and the displacement of the ridge to the west. On May 9, the study area was in a low-gradient field, while the flow changed to a northern, relatively

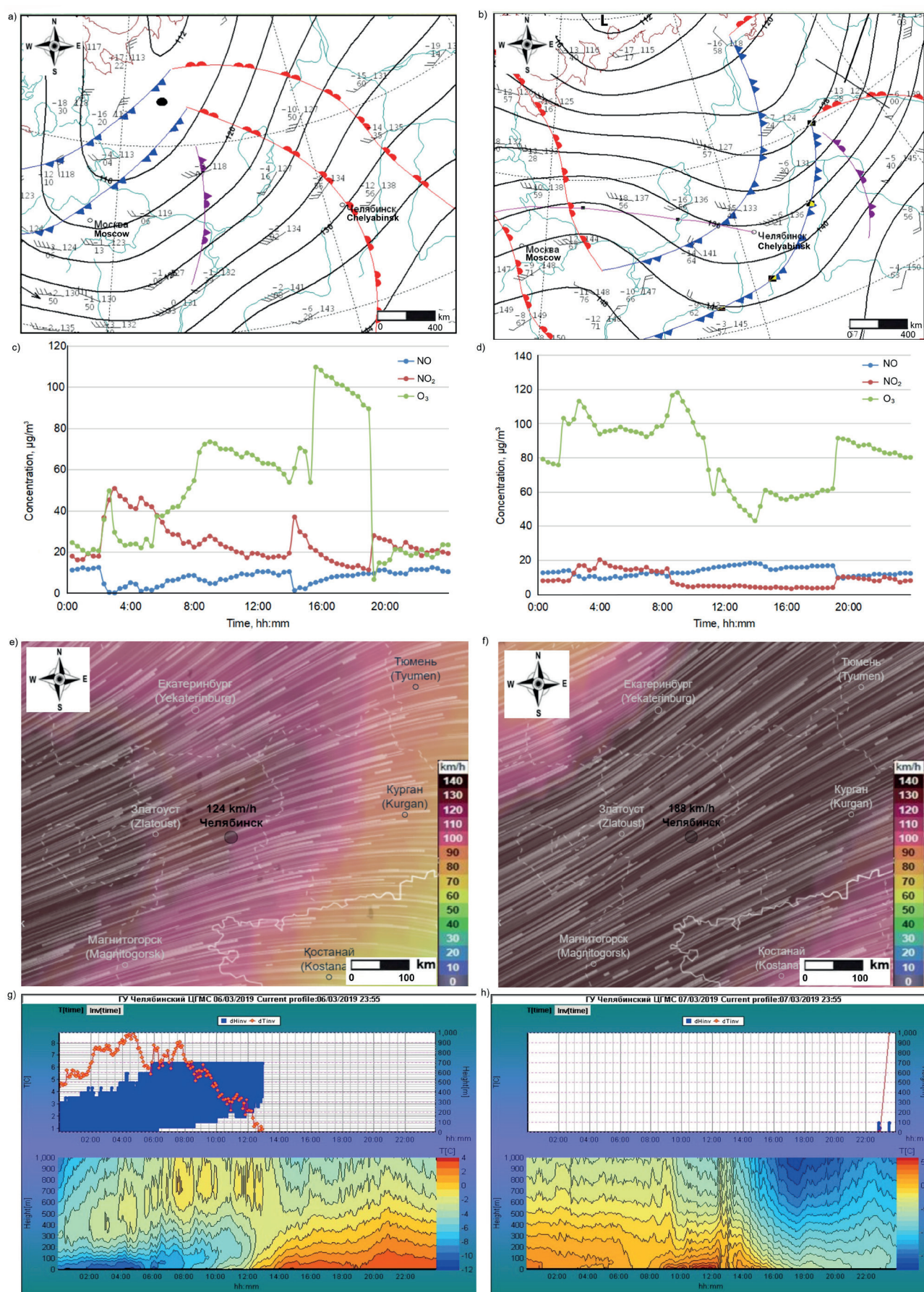


Fig. 6. Weather charts at 850 hPa; hourly variation of NO, NO₂ and O₃ concentrations (µg·m⁻³); 300 hPa charts with wind speed and wind vectors; and temperature profiles on March 6 (left) and March 7 (right)

weak 9–16 m·s⁻¹ (32–58 km·h⁻¹). The crest corresponded to an extensive Siberian anticyclone at ground level and up to 1.5 km on May 8. On May 9, a local cyclone formed in Bashkiriya on the wave of the polar front, which brought rain to the Chelyabinsk region. The temperature background remained

almost unchanged, then the pressure increased again and Chelyabinsk found itself on the crest of an anticyclone. The wind at the ground was weak: calm or variable 1–3 m·s⁻¹; only on May 9 gusts of up to 15 m·s⁻¹ were observed. Abnormally hot weather was observed with a deviation of average daily

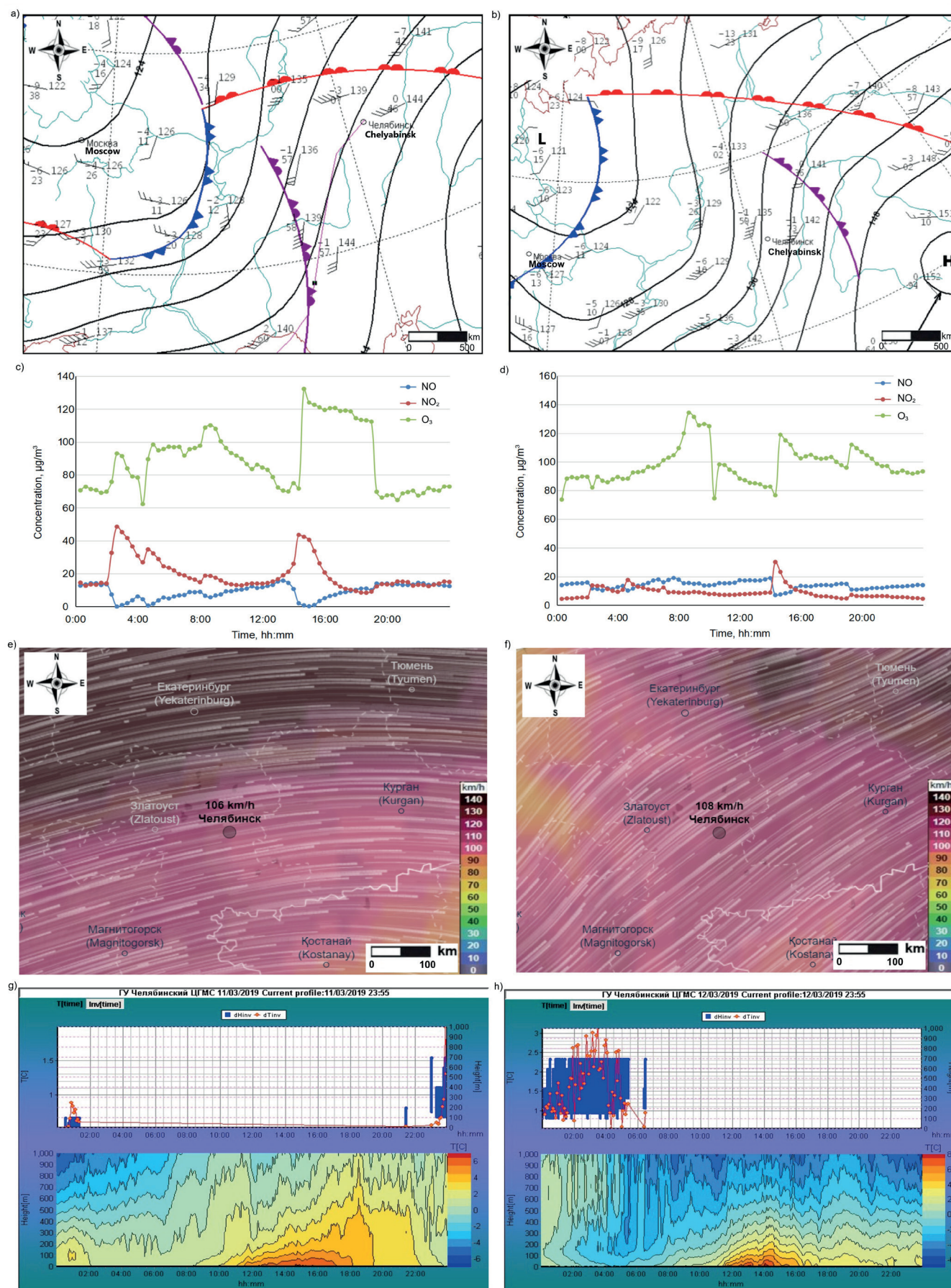


Fig. 7. Weather charts at a level of 850 hPa, hourly variation of NO, NO₂, and O₃ concentrations ($\mu\text{g}/\text{m}^3$), 300 hPa charts with wind speed and wind vectors and temperature profiles on March 11 (left) and 12 (right)

temperatures from the norm by 7–12 °C; the maximum air temperature in the city reached +28 °C. Nighttime and daytime inversions were also observed.

There were days with strong sunlight and low winds, which favored the photochemical production of O₃ and the accumulation of O₃ and its precursors. Photochemical O₃ formation is the cause of the observed high concentration of O₃.

Episode 4

On June 10–11, high O_3 concentrations of up to $160 \mu\text{g}\cdot\text{m}^{-3}$ were recorded throughout the day. At the level of 300 hPa (≈ 9 km) at the beginning of the period, the Chelyabinsk region was on the northeastern periphery of

the altitudinal ridge; by the end of the period, an extensive tropospheric trough was spreading from the territory of the island of Novaya Zemlya and the Kara Sea and covered the Chelyabinsk region. The flows were northwest $12\text{--}16 \text{ m}\cdot\text{s}^{-1}$ ($43\text{--}58 \text{ km}\cdot\text{h}^{-1}$). At the level of 850 hPa (≈ 1.5 km),

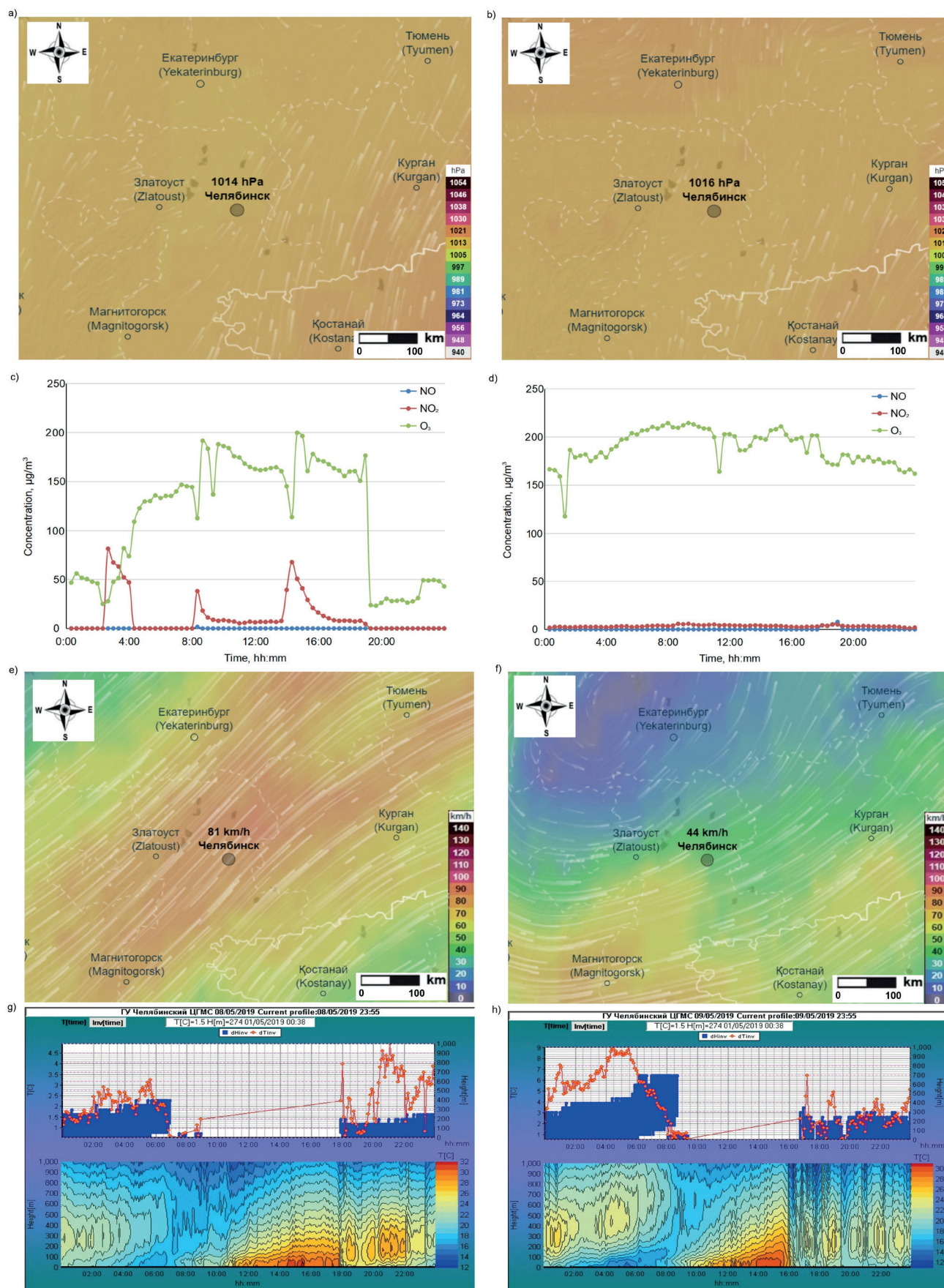


Fig. 8. Synoptic weather charts with the surface air pressure and wind vectors, hourly variation of NO, NO₂, and O₃ concentrations ($\mu\text{g}\cdot\text{m}^{-3}$), 300 hPa charts with wind speed and wind vectors, and temperature profiles on May 8 (left) and May 9 (right)

the territory was in the warm sector of the crest of a vast anticyclone with its center south of Moscow. There was an occlusion front and a cold front in the warm sector, so there were heavy rains in the Chelyabinsk region on June 10–11. During this period, the temperature background in Chelyabinsk was high; maximum air temperatures reached 26–28 °C; night inversions were also observed. The night was calm; during the day, there was a west/northwest wind of 3–5 m·s⁻¹, with isolated gusts of 11–12 m·s⁻¹. At the level

of 925 hPa, a moderate wind of a western, northwestern direction of 7–10 m·s⁻¹ was observed (Fig. 9).

In hot, windless weather on the afternoon of June 10, a photochemical accumulation of O₃ occurred. At 4 p.m., after the passage of a cold front and local rainfall, a sharp decrease in O₃ concentration in the air occurred in the area of the monitoring station. On the night of June 10–11, warm, windless weather returned. Under nighttime inversion conditions, air from O₃-rich areas on the outskirts

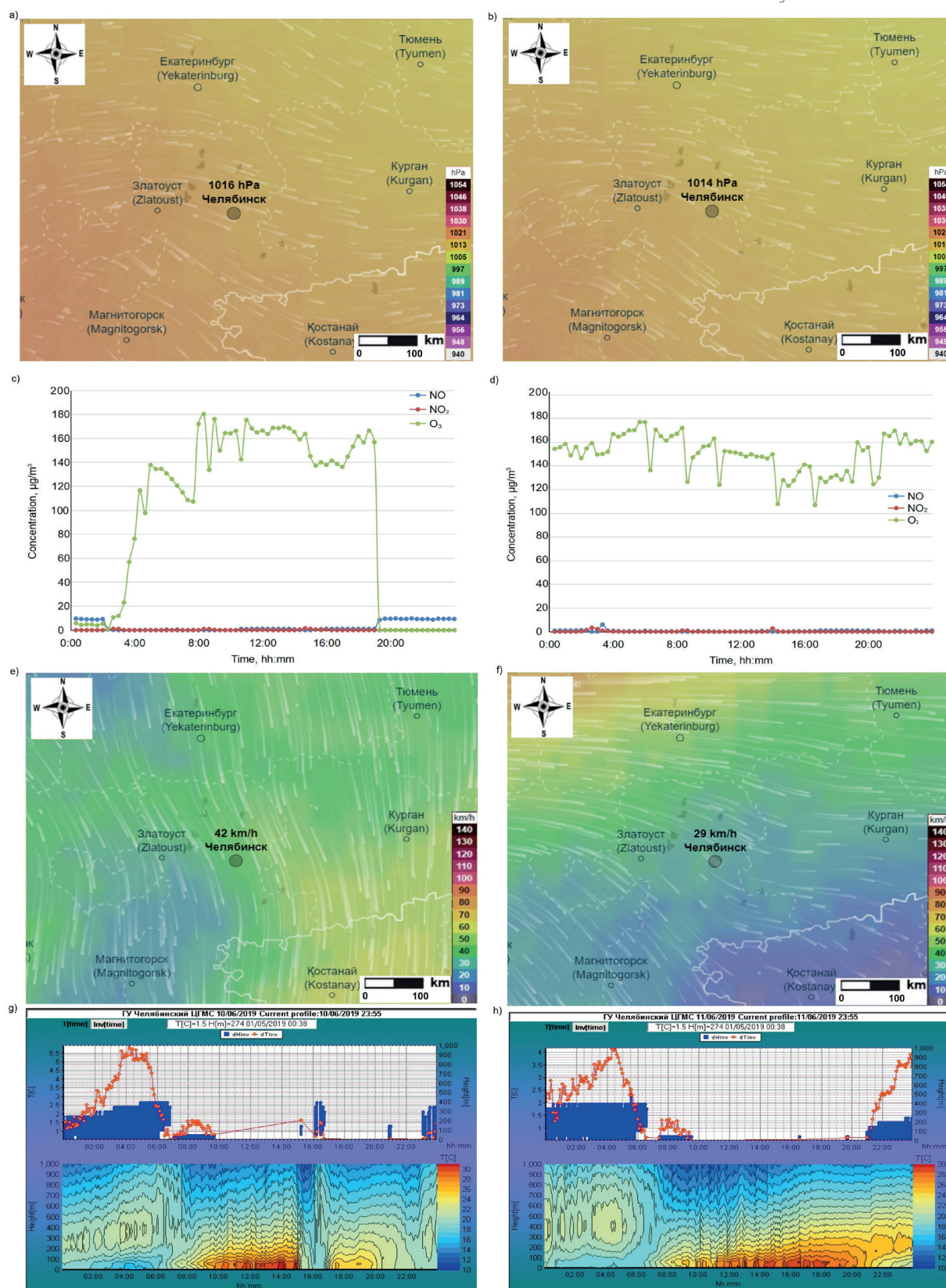


Fig. 9. Synoptic weather charts with the surface air pressure and wind vectors, hourly variation of NO, NO₂ and O₃ concentrations (µg·m⁻³), 300 hPa charts with wind speed and wind vectors, and temperature profiles on June 10 (left) and June 11 (right)

entered the center, causing the O_3 concentration to increase again. With the anticyclone on June 11, hot weather set in, which contributed to the photochemical accumulation of O_3 . High concentrations of surface O_3 were observed throughout the entire day on June 11.

CONCLUSION

This study investigates the processes associated with ground-level O_3 in a typical Russian industrial city, Chelyabinsk, including O_3 content and its relationship with atmospheric dynamics and chemical processes. We offer the following conclusions and recommendations:

- The data clearly show severe O_3 pollution in the city at a background station. To obtain a complete picture of pollution, data from other (in particular industrial and transport) monitoring stations is needed. In this regard, the expansion of the city's air monitoring network is strongly recommended.

- Measurements and studies have shown that O_3

production is correlated with NO_x . However, strategies need to be developed to control O_3 precursors, particularly VOCs. It is recommended to accelerate the implementation of VOC and NO_x control measures.

- It has been established that vertical mixing and transport by LLJs is one factor in the increase in O_3 in the spring (the March maximum). In summer (the June maximum), it is due to photochemical reactions. It is recommended that control measures be taken to reduce emissions from the energy and vehicle industries.

- Global transport appears to be an important cause of the high O_3 levels in Chelyabinsk, highlighting the need for precursor controls in other major cities as well as control of transboundary transport, including from Kazakhstan.

- Additional vertical measurements of chemical and meteorological parameters are needed to understand processes throughout the boundary layer and exchanges with the free troposphere.

- Further research on the effects of O_3 on human health and crops is recommended.

REFERENCES

- Andreev V.V., Arshinov M.Y., Belan B.D., Davydov D.K., Elansky N.F., Zhamsueva G.S. et al. (2021). Surface ozone concentration over Russian territory in the first half of 2020. *Atmospheric and Oceanic Optics*, 33(6), 671-681, DOI: 10.1134/S1024856020060184.
- Andreev V.V., Arshinov M.Y., Belan B.D. et al. (2022). Tropospheric ozone concentration on the territory of Russia in 2021. *Atmospheric and Oceanic Optics*, 35(6), 741-757, DOI: 10.1134/S1024856022060033.
- Antokhin P.N., Antokhina O.Yu., Antonovich V.V., Arshinova V.G., Arshinov M.Yu., Belan B.D., Belan S.B., Davydov D.K., Dudorova N.V., Ivlev G.A., Kozlov A.V., Pestunov D.A., Rasskazchikova T.M., Savkin D.E., Simonenkov D.V., Sklyadneva T.K., Tolmachev G.N., Fofonov A.V. (2020). Correlation between the dynamics of atmospheric composition and meteorological parameters near Tomsk. *Atmospheric and Oceanic Optics*, 33(7), 529-537. DOI: 10.15372/AOO20200705
- Belan B.D. (2010). *Ozone in the troposphere*. Tomsk: Publishing House of the Institute of Atmospheric Optics SB RAS.
- Berezina E., Moiseenko K., Skorokhod A., Pankratova N.V., Belikov I., Belousov V. and Elansky N.F. (2020). Impact of VOCs and NO_x on ozone formation in Moscow. *Atmosphere*, 11, 1262, DOI: 10.3390/atmos11111262.
- Chubarova N.Ye., Androsova Ye.Ye., and Lezina Ye.A. (2021). The dynamics of the Atmospheric pollutants during the Covid-19 Pandemic 2020 and their relationship with meteorological conditions in Moscow. *Geography, Environment, Sustainability*, 14(4), DOI: 10.24057/2071-9388-2021-012.
- Colombi N.K., Jacob D.J., Yang L.H., Zhai S., Shah V. et al. (2023). Why is ozone in South Korea and the Seoul metropolitan area so high and increasing? *Atmospheric Chemistry and Physics*, 23, 4031-4044. DOI: 10.5194/acp-23-4031-2023.
- Di Bernardino A., Mevi G., Iannarelli A.M., Falasca S., Cede A., Tiefengraber M. and Casadio S. (2023). Temporal variation of NO_2 and O_3 in Rome (Italy) from Pandora and in situ measurements. *Atmosphere*, 14(3), 594, DOI: 10.3390/atmos14030594.
- Fallmann J., Forkel R. and Emeis S. (2016). Secondary effects of urban heat island mitigation measures on air quality. *Atmospheric Environment*, 125, 199-211, DOI: 10.1016/j.atmosenv.2015.10.094.
- Geng F., Tie X., Guenther A., Li G. et al. (2011). Effect of isoprene emissions from major forests on ozone formation in the city of Shanghai, China. *Atmospheric Chemistry and Physics*, 11, 10449-10459, DOI: 10.5194/acpd-11-18527-2011.
- Kim S., Sanchez D., Wang M., Seco R. et al. (2016). OH reactivity in urban and suburban regions in Seoul, South Korea - an East Asian megacity in a rapid transition. *Faraday Discussions*, 18(189), 231-51, DOI: 10.1039/c5fd00230c.
- Knight T., Price S., Bowler D. et al. (2021). How effective is 'greening' of urban areas in reducing human exposure to ground-level ozone concentrations, UV exposure and the 'urban heat island effect'? An updated systematic review. *Environmental Evidence*, 10, 12, DOI: 10.1186/s13750-021-00226-y.
- Krupnova T.G., Rakova O.V., Plaksina A.L., Gavrilkina S.V., Baranov E.O. and Abramyan A.D. (2020). Effect of urban greening and land use on air pollution in Chelyabinsk, Russia. *Biodiversitas*, 21, 2716-2720. DOI: 10.13057/biodiv/d210646.
- Lee K.-Y., Kwak K.-Y., Ryu Y.-H., Lee S.-H. and Baik J.-J. (2014). Impacts of biogenic isoprene emission on ozone air quality in the Seoul metropolitan area. *Atmospheric Environment*, 96, 209-219, DOI: 10.1016/j.atmosenv.2014.07.036.
- McGenity T.J., Crombie A.T. and Murrell J.C. (2018). Microbial cycling of isoprene, the most abundantly produced biological volatile organic compound on Earth. *International Society for Microbial Ecology*, 12, 931-941, DOI: 10.1038/s41396-018-0072-6.
- Moiseenko K.B., Vasileva A.V., Skorokhod A.I., Belikov I.B., Repin A.Yu. and Shtabkin Yu.A. (2021). Regional impact of ozone precursor emissions on NO_x and O_3 levels at ZOTTO tall tower in central Siberia, *Earth Space Sci*, 8, 2021EA001762, DOI: 10.1029/2021EA001762.
- Nuvolone D., Petri D. and Voller F. (2018). The effects of ozone on human health. *Environmental Science and Pollution Research*, 25(5), DOI: 10.1007/s11356-017-9239-3.
- Nguyen D.-H., Lin Ch., Vu C.-T., Cheruiyot N.K., Nguyen M.K., Le T.H., Lukkhasorn W., Vo T.-D.-H. and Bui X.-T. (2022). Tropospheric ozone and NO_x : A review of worldwide variation and meteorological influences. *Environmental Technology and Innovation*, 28, 102809, DOI: 10.1016/j.eti.2022.102809.
- Ouyang S., Deng T., Liu R. et al. (2022). Impact of a subtropical high and a typhoon on a severe ozone pollution episode in the Pearl River Delta, China. *Atmospheric Chemistry and Physics*, 22, 10751-10767, DOI: 10.5194/acp-22-10751-2022.
- Rawat K. and Matta G. (2021). Ozone: Risk assessment, environmental, and health hazard. In: Singh J(ed) *Hazardous Gases: Risk Assessment on Environment and Human Health*, Academic Press, 301-312.

- Ren X., Wen Y., He Q., Cui Y. et al. (2021). Higher contribution of coking sources to ozone formation potential from volatile organic compounds in summer in Taiyuan, China. *Atmospheric Pollution Research*, 12(6), 101083, DOI: 10.1016/j.apr.2021.101083.
- Rosenkranz M., Chen Y., Zhu P. and Vlot A.C. (2021). Volatile terpenes - mediators of plant-to-plant communication. *Plant*, 108(3), 617-631, DOI: 10.1111/tpj.15453.
- Salonen H., Salthammer T. and Morawska L. (2018). Human exposure to ozone in school and office indoor environments. *Environment International*, 119, 503-514, DOI: 10.1016/j.envint.2018.07.012.
- Simakina T.E. and Kryukova S.V. (2020). Spatio-temporal distribution of surface ozone in Saint Petersburg, *Gidrometeorologiya i Ekologiya. Hydrometeorology and Ecology*, 61, 407-420 (In Russian), DOI: 10.33933/2074-2762-2020- 61-407-420.
- Simon H., Fallmann J., Kropp T., Tost H. and Bruse M. (2019). Urban trees and their impact on local ozone concentration-a microclimate modeling study. *Atmosphere*, 10(3), 154, DOI: 10.3390/atmos10030154.
- Thorp T., Arnold S.R., Pope R.J., Spracklen D.V. et al. (2021). Late-spring and summertime tropospheric ozone and NO₂ in Western Siberia and the Russian Arctic: regional model evaluation and sensitivities. *Atmospheric Chemistry and Physics*, 21, 4677-4697, DOI: 10.5194/acp-21-4677-2021.
- Virolainen Ya.A., Ionov D.V. and Polyakov A.V. (2023). Analysis of long-term measurements of tropospheric ozone at the St. Petersburg State University Observational site in Peterhof, *Izvestiya, Atmospheric and Oceanic Physics*, 59(3), 287-295, DOI: 10.1134/S000143382303009X.
- Wang J., Dong J., Guo J., Cai P., Li R., Zhang X., Xu Q. and Song X. (2023). Understanding temporal patterns and determinants of ground-level ozone. *Atmosphere*, 14(3), 604, DOI: 10.3390/atmos14030604.
- Watson L., Wang K.-Y., Hamer P. and Shallcross D. (2006). The potential impact of biogenic emissions of isoprene on urban chemistry in the United Kingdom. *Atmospheric Science Letters*, 7, 96-100, DOI: 10.1002/asl.140.
- Xie Y., Cheng Ch., Wang Z., Wang K., Wang Yu. et al. (2021). Exploration of O₃-precursor relationship and observation-oriented O₃ control strategies in a non-provincial capital city, southwestern China. *Science of the Total Environment*, 800, 149422, DOI: 10.1016/j.scitotenv.2021.149422.
- Zhang J., Wei Y. and Fang Z. (2019). Ozone pollution: a major health Hazard worldwide. *Frontiers in Immunology*, 10, 2518, DOI: 10.3389/fimmu.2019.02518.